Published in final edited form as:
Oncogene. 2010 December 2; 29(48): 6367–6377. doi:10.1038/onc.2010.364.

Insulin-like growth factor 1 receptor antibody induces rhabdomyosarcoma cell death via a process involving AKT and Bcl-x_L

LH Mayeenuddin[1,2], **Y Yu**[1,2], **Z Kang**[1,2], **LJ Helman**[3], and **L Cao**[1]

[1]Genetics Branch, Center for Cancer Research, National Cancer Institute, Bethesda, MD, USA

[2]Laboratory of Proteomics and Analytical Technologies, SAIC-Frederick, Inc., NCI-Frederick, Frederick, MD, USA

[3]Pediatric Oncology Branch, Center for Cancer Research, National Cancer Institute, Bethesda, MD, USA

Abstract

Insulin-like growth factors (IGFs) and their receptor, IGF-1 receptor (IGF1R), have important roles in growth, development, stress response, aging and cancer. There are many agents that inhibit IGF1R in oncology clinical development, and in some cases, they have been associated with rapid tumor regression. However, it is not clear by which process these targeted agents induce cancer cell death and how to predict such tumor responses. Here, we showed that IGF1R antibody led to rapid cell death and tumor regression in some rhabdomyosarcoma (RMS) cells. Mechanistic analysis revealed a rapid onset of mitochondrial-dependent apoptosis, including mitochondrial depolarization, cytochrome C release and the activation of specific caspases. The antibody sensitive cells had greater dependence on AKT for maintaining downstream signaling and the expression of a constitutively active *AKT*, which restored AKT-signaling in these cells, inhibited anti-IGF1R induced cell death. Further analysis showed IGF1R antibody-induced hypophosphorylation of BAD and activation of downstream BAX. Interestingly, the examination of RMS cell lines and tumors revealed an inverse correlation between elevated IGF1R and Bcl-2 level ($P = 0.033$), with the sensitive cells lacking Bcl-2 expression. The overexpression of BAD specific target, Bcl-x_L, conferred resistance, whereas Bcl-x_L knockdown sensitized cells lacking Bcl-2 to anti-IGF1R-induced cell death. We propose that RMS pathogenesis involves increased IGF1R expression that enhances AKT and Bcl-x_L-mediated cell survival, and the blockage of IGF1R results in inhibition of survival signal from Bcl-x_L and cell death in the sensitive Bcl-2 negative cells.

Keywords

IGF1R therapeutic antibody; apoptosis; tumor regression; predictive biomarker; Bcl-x_L; Bcl-2

Correspondence: Dr L Cao, Genetics Branch, Center for Cancer Research, National Cancer Institute, 37 Convent Dr., MSC 4265, Building 37, Room 6134, Bethesda, MD 20892-4265, USA. caoli@mail.nih.gov.

Conflict of interest

The authors declare no conflict of interest.

Supplementary Information accompanies the paper on the Oncogene website (http://www.nature.com/onc)

Introduction

Signaling through insulin-like growth factor 1 receptor (IGF1R) is an established survival or proliferation-pathway in many systems (Kooijman, 2006; Kurmasheva and Houghton, 2006). Studies using interleukin (IL)-3-dependent hemopoietic cell lines demonstrated that IGF-1 could delay and suppress apoptosis when cells were deprived of IL-3 (Rodriguez-Tarduchy *et al.*, 1992). In addition, IGFs have also been shown to protect cells from cell death induced by serum-deprivation, as well as a wide range of intrinsic and extrinsic death stimuli (Kurmasheva and Houghton, 2006).Many studies have shown that the activation of IGF1R results in the stimulation of multiple cellular signaling cascades, particularly AKT and mitogen-activated protein kinase pathways (Kooijman, 2006; Kurmasheva and Houghton, 2006). Activated AKT has been strongly associated with the inhibition of apoptosis through the phosphorylation of various cellular proteins, including BAD, FKHR, NF-κB, and MDM2 (Hennessy *et al.*, 2005; Manning and Cantley, 2007). It is of particular relevance that a previous study showed a strong correlation between IGF1R-mediated survival and phosphorylation of BAD with a series of *IGF1R* mutants expressed in D32 murine hematopoeitic cells deprived of IL-3 (Peruzzi *et al.*, 1999). However, it is less clear whether IGF1R itself is specifically required for cancer cell survival and, why that may be so. Such understanding is important for single agent anti-IGF1R therapy.

Owing to the important roles of IGF1R in proliferation, survival and cancer, a large number of investigational agents targeting IGF1R are being developed for cancers and a majority of them are monoclonal antibodies against the receptor (Clemmons, 2007; Gualberto and Pollak, 2009). Although anti-IGF1R antibodies are highly specific, and are capable of downregulating the receptor and inhibiting tumor growth in xenograft models (Burtrum *et al.*, 2003; Sachdev *et al.*, 2003; Cohen *et al.*, 2005; Goetsch *et al.*, 2005; Wang *et al.*, 2005; Wu *et al.*, 2005), little is known about their ability to kill tumor cells or the underlying mechanism. Interestingly, early clinical studies with the antibodies have shown that they are generally safe (Haluska *et al.*, 2007; Gualberto and Pollak, 2009). More importantly, single agent activities of anti-IGF1R has been observed within some of the trials (Gualberto and Pollak, 2009; Tolcher *et al.*, 2009), suggesting that IGF1R antibody alone can be sufficient to induce cancer cell death. Thus, it becomes very important to understand such a specific dependence on IGF1R for cancer cell survival and the mechanism of action for IGF1R targeted agents. Such studies may provide the basis for the selective action of anti-IGF1R therapies and allow the identification of predictive biomarkers for these agents.

Rhabdomyosarcoma (RMS) is a rare pediatric sarcoma that arises from skeletal muscle, and is highly malignant and metastatic. Our previous study suggests that elevated IGF1R level is predictive of the anti-proliferative response of an anti-IGF1R antibody (Cao *et al.*, 2008). In this report, we show that an antibody against IGF1R is capable of inducing rapid apoptosis and tumor regression in RMS. Our data indicate an inverse correlation between IGF1R and Bcl-2 in RMS cells and that IGF1R antibody induces cancer cell death in some Bcl-2 negative cells, mediated via mitochondrial-dependent apoptosis, involving AKT and Bcl-x_L. Overexpression of constitutively active AKT or Bcl-x_L significantly inhibits anti-IGF1R induced apoptosis, whereas small interfering RNA against Bcl-x_L sensitizes Bcl-2 negative cells to anti-IGF1R. Thus, we suggest that elevated IGF1R is a pathogenic factor for RMS, enabling their survival via upregulating Bcl-x_L activity, in tumors cells lacking Bcl-2. Such specific dependence on elevated levels of IGF1R for survival makes them particularly susceptible to anti-IGF1R based therapies.

Results

Anti-IGF1R antibody is capable of inducing rapid apoptotic cell death and tumor regression

We screened 13 RMS cell lines for their sensitivity to an IGF1R therapeutic antibody h7C10 (MK0646, Merck, Rahway, NJ, USA). Three of the cell lines (Rh4, Rh41 and CTR) were very sensitive to the antibody; and interestingly they also expressed the highest levels of IGF1R, as determined by an IGF1R immunoassay (data not shown). Rh41 exhibited a high degree of sensitivity to h7C10 with significantly reduced cell viability (Figure 1a). In contrast, h7C10 only had modest growth inhibitory effect on RD cells. The IGF1R antibody-induced Rh41 cell death was verified with microscopic examination with significant cell detachment within 6 h of antibody addition (data not shown). After 3 days of h7C10 treatment, most of the h7C10-treated sensitive Rh41 cells were dead (Supplementary Figure S1), whereas no dead cells were visible with h7C10-treated resistant Rh18. Clonogenic assay results further confirmed this observation of anti-IGF1R induced rapid cell death, in which cells were treated with h7C10 for 3 days, and then incubated with fresh media without the antibody for 2 weeks (Figure 1b, Supplementary Figure S1). Dose-dependent sensitivity study was performed to determine the potency of anti-IGF1R. The results showed that the IC_{50} against Rh41 and Rh4 were at ~3–8 ng/ml (Figure 1c). h7C10 had very limited activity toward Rh18 and RD cells, in which the IC_{50} could not be established as the growth was inhibited by <30%. We further demonstrated this anti-IGF1Rdependent cell death using another monoclonal antibody R1507 (Roche, Nutley, NJ, USA) with very similar potency and selectivity (data not shown). The results show that Rh41 and Rh4 are selectively sensitive to IGF1R antibodies in complete culture medium.

To better characterize h7C10-induced cell death, we performed terminal deoxynucleotidyl transferase dUTP nick end labeling (Tunel) assay with Rh41 and RD cells. After 2 days, the majority of h7C10-treated Rh41 cells were Tunel positive, associated with condensed nuclei with 4′-6-diamidino-2-phenylindole staining and cleaved poly ADP ribose polymerase (PARP) (Figure 1d). No Tunel positive cell or PARP cleavage was seen with RD cells (Figure 1d). In another example, h7C10 was also able to induce apoptosis of Rh4 cells (Supplementary Figure S2). Our results indicate that anti-IGF1R antibody induces apoptotic cell death in susceptible RMS cells expressing high levels of IGF1R.

In vivo xenograft study was performed to determine the effects of anti-IGF1R on the sensitive Rh41 cells. The antibody treatment was initiated when the tumors reached about 5mm in size and continued for a total of 3 weeks. Apparent tumor regression was visible after 4 days of h7C10 treatment and the tumors essentially disappeared after 2 weeks of treatment with Rh41 cells (Figure 2a). In comparison, h7C10 treatment only resulted in modest growth inhibition for RD cells. Western blot analysis revealed the effects of h7C10 in downregulating IGF1R (Figure 2b). Thus, h7C10 selectively results in almost complete tumor regression of sensitive Rh41 cells.

To determine if the effect of anti-IGF1R was durable, the antibody treatment was stopped after 3 weeks of treatment. The results showed that the growth of the Rh41 xenograft tumors resumed and eventually all reached the maximal size (Figure 2a) pre-defined in our experimental protocol. The results suggest the presence of residual viable tumor cells and the need of continuous treatment.

Anti-IGF1R induces intrinsic apoptosis via a mitochondrial-dependent pathway

We examined the mechanism of h7C10-induced apoptosis with a mitochondrial potential fluorescent cationic dye, JC-1. In healthy cells, JC-1 accumulates in the mitochondria as aggregates that fluoresce red. In apoptotic cells, the mitochondrial membrane potential

collapses, and JC-1 enters the cytoplasm in a monomeric form where it fluoresces green. Depolarization of mitochondria is an important feature of mitochondrial-dependent programmed cell death (Jiang and Wang, 2004). Confocal microscopy results showed a marked induction of mitochondrial depolarization after 24 h of h7C10 treatment of Rh41 (Figure 3a). Fluorescence-activated cell sorting (FACS) analysis further confirmed that a significantly higher percentage of h7C10-treated cells were depolarized than untreated control (Figure 3b). Cytochrome C is a key mediator of mitochondrial-dependent apoptosis (Jiang and Wang, 2004). Our results indicated that cytochrome C was released into the cytosolic fraction visible via immunoblot within 4 h of antibody treatment (Figure 3c). The cytosolic fractionation was confirmed with the absence of a mitochondria specific voltage-dependent anion channel protein. The biological effects of the released cytochrome C was further confirmed with the analysis of cleaved caspase 9 and caspase 3 in h7C10 treated cells at as early as 4 h (Figure 3d), characteristic of cytochrome C-dependent programmed cell death. Thus, our data suggest that anti-IGF1R-induced cell death in RMS cells is mediated through mitochondrial-dependent apoptosis.

AKT is implicated in anti-IGF1R induced cell death

To understand the mechanism of anti-IGF1R-induced mitochondrial-mediated apoptosis, we examined the events upstream of cytochrome C release. Treatment with h7C10 resulted in the downregulation of IGF1R in Rh41 and RD cells (Figure 4a). The IGF1R antibody led to rapid and significantly reduced p-AKT at T308 and S473 residues in both cell lines, yet it had virtually no detectable effect on p-ERK (Figure 4b). Furthermore, the reduced p-AKT was associated with the selective inhibition of AKT signaling only in the sensitive Rh41 cells, as demonstrated by the hypophosphorylation of a number of downstream target proteins, including p-GSK3β, p-mTOR, p-EIF4EBP1 and p-S6RP (Figure 4b). The introduction of a constitutively active myr-*AKT* via adenovirus resulted in increased p-AKT that was no longer inhibited by h7C10 in Rh41 cells (Figure 4c). When the cells were treated with h7C10, the myr-*AKT* virus infected Rh41 cells were noticeably more resistant to h7C10 than the cells infected by the control virus (Figure 4d). Therefore, the inhibition of AKT signaling is important in mediating the cytotoxic activity of anti-IGF1R.

Anti-IGF1R antibody activates pro-apoptotic BAD and BAX

In anti-IGF1R treated Rh41 cells, we also observed a significant reduction of p-BAD (Figure 5a), which was shown to be important for maintaining the mitochondrial threshold for apoptosis (Datta *et al.*, 2002). To continue the mechanistic investigations, we examined the events downstream of BAD and our data showed that h7C10 induced the oligomerization of pro-apoptotic BAX protein (Figure 5b). BAX has a critical role in mediating cytochrome C release through oligomerization (Adams and Cory, 2007). It has been shown to accelerate the opening of voltage-dependent anion channel, thus allowing cytochrome C release (Shimizu *et al.*, 1999). Our results show that h7C10 induces the hypophosphorylation of BAD and oligomerization of BAX; and as noted both of these processes have previously been shown to be associated with cytochrome C release and apoptosis.

Involvement of Bcl-x_L in IGF1R antibody-induced apoptosis

We further explored the links between activated BAD and BAX in order to understand the selective action of anti-IGF1R. Of all the Bcl-2 family of pro-survival proteins, Bcl-x_L has been specifically implicated as a critical link between BAD- and BAX-mediated cytochrome C release (Yang *et al.*, 1995; Muslin *et al.*, 1996; Zha *et al.*, 1996; Yaffe *et al.*, 1997). Given the delicate interplay between pro- and anti-apoptotic proteins, which determine cell survival, we decided to investigate the expression levels of a number of pro- and anti-apoptotic proteins in RMS. The examination of the expression profile of pro-survival Bcl

proteins revealed that Mcl-1 was similarly expressed in a panel of RMS cell lines. Bcl-2, however, was largely non-detectable in the sensitive Rh41 and Rh4 cells (Figure 6a), suggesting that Bcl-x_L maybe more important in mediating the survival signal from IGF1R. As the level of Bcl-x_L in Rh41 was lower than other RMS cell lines, we asked if increased expression of Bcl-x_L would be sufficient to inhibit anti-IGF1R induced cell death. *Bcl-x_L* was introduced into Rh41 cells via lentiviral-mediated gene transfer (Barcia *et al.*, 2007). Protein expression analysis showed a several fold increase in Bcl-x_L in *Bcl-x_L* lentivirus infected cells (Figure 6b). When Rh41-*Bcl-x_L* and Rh41-vec cells were treated with h7C10, *Bcl-x_L* transgene suppressed h7C10-induced PARP cleavage, but had no effect on h7C10-mediated inhibition of AKT signaling (Figure 6c). FACS analysis of the cells treated with anti-IGF1R showed a complete inhibition of h7C10-induced apoptosis in Rh41 by the exogenous expression of *Bcl-x_L* (Figure 6d). RNA interference experiments further supported the involvement of Bcl-x_L in anti-IGF1R induced cell death in RMS. When Bcl-2 negative CTR cells (Figure 8b) were transfected with siBcl-x_L to reduce the level of Bcl-x_L (Figure 5e), they were substantially more susceptible to h7C10-induced cell death ($P < 0.001$, Figure 6f). In comparison, the sensitivity of Bcl-2 positive RD cells to h7C10 was not affected by siBcl-x_L ($P = 0.861$, Figure 6f). The results suggest that when Bcl-2 is absent, the levels of Bcl-x_L become critical in determining RMS survival when they are treated with an IGF1R antibody to downregulate its signaling.

As Bcl-x_L transgene prevented anti-IGF1R-induced cell death, we asked if it would allow cells to grow in the presence of the antibody. Such understanding is important, as it implies potentially a dual role of elevated IGF1R in tumor pathogenesis. Our results showed that although Rh41-*Bcl-x_L* cells exhibited little cell death following anti-IGF1R treatment, they were growth-inhibited by the antibody (Figure 7a). Further time course analysis indicated that Rh41-*Bcl-x_L* cells were still completely susceptible to h7C10-mediated growth inhibition in proliferation assays (Figure 7b). Thus, the results indicate the dual function of IGF1R in suppressing apoptotic death and in enabling proliferative growth of RMS cells.

Inverse correlation between IGF1R and Bcl-2 levels suggests two strategies leading to the survival of RMS cells

Previous studies showed that IGF-1 may be involved in upregulating the expression of Bcl-2 family proteins (Minshall *et al.*, 1997; Parrizas and LeRoith, 1997; Zhang and D'Ercole, 2004). As IGF1R activation resulted in increased BAD phosphorylation and its inactivation led to activated Bcl-x_L, it would appear to be redundant for IGF1R to also induce the expression of Bcl-2 family proteins. Our study using h7C10 to inhibit IGF1R showed that the antibody did not downregulate Bcl-2 and Bcl-x_L in RD cells that expressed higher levels of both proteins (Figure 8a). Thus, data suggest that in RD cells, the elevated levels of Bcl-2 and Bcl-x_L are independent of IGF1R activation status.

Our results showed a large variation in the expression of Bcl-2 in RMS cell lines (Figure 6a). The follow-up analysis of the expression of Bcl family genes in 10 RMS cell lines revealed modest variation in Bcl-x_L, with the lowest level in Rh41, a cell line that was most sensitive to h7C10 (Figure 8b). Strikingly, Bcl-2 was almost completely absent in cell lines with high levels of IGF1R, including Rh4, Rh30, Rh41 and CTR. Of seven RMS cell lines with moderate to high IGF1R, six have little or no Bcl-2. In contrast, Bcl-2 was expressed at the highest levels in all three resistant cell lines with lowest IGF1R, including Rh1, Rh18 and Rh36 (Figure 8b). Fisher's exact test on the levels of Bcl-2 and IGF1R showed a potentially significant inverse correlation between the expression levels of these two proteins with $P = 0.033$. We further evaluated such inverse correlation on the expression levels of IGF1R and Bcl-2 in RMS tumors. Of eight RMS tumors examined, all three tumors with low IGF1R expressed high levels of Bcl-2, whereas four out of five tumors with high IGF1R had no detectable Bcl-2, again confirming such potential correlation between the

levels of these two proteins (Figure 8c). In summary, these data suggest an inverse relationship between IGF1R and Bcl-2 expression in RMS and that the elevated IGF1R may provide an alternative survival strategy to Bcl-2 overexpression during RMS pathogenesis.

Discussion

Induction of tumor regression is the most important primary end point in the early stage development of investigational therapeutics. There is very significant interest in targeting IGF1R with close to 30 agents currently under investigation, of which several therapeutic antibodies have already been shown to result in partial or complete responses in patients (Gualberto and Pollak, 2009). Whilst IGFs and IGF1R are very important in protecting cells from growth factor deprivation and a wide range of intrinsic and extrinsic stimuli, the reports on the activities of these investigational IGF1R antibodies have been largely limited to growth inhibition in preclinical models and little is reported on cell death or tumor regression induced by these therapeutic antibodies. By using RMS as a model system, we show that a therapeutic IGF1R antibody, h7C10, induces acute cell death *in vitro*. This anti-IGF1R-mediated cell death was confirmed using another IGF1R therapeutic antibody, R1507. *In vivo*, h7C10 selectively leads to tumor regression of the sensitive Rh41 cells, yet, only exhibits growth inhibitory activity against more resistant RD cells. As tumor regression is critically important in clinical investigations for single-agent therapies, the model presented here should have value in evaluating and selecting IGF1R targeted agents for clinical studies. It is also worth noting that despite the apparent near complete regression of the sensitive tumors in the xenograft model, the continuous administration of the IGF1R antibody is essential to maintain this effect. This result reflects the initial clinical experiences with IGF1R antibodies and such a model may facilitate the investigation of the escape mechanism and the exploration of combination therapy targeting the residual tumor cells.

Two important issues in the development of the IGF1R targeted agents are the understanding of the mechanism of selective action and the identification of predictive biomarkers that can be implemented in the correlative studies during the trials. The availability of suitable cell line pairs and a highly selective IGF1R antibody allowed us to explore the possible mechanism associated with anti-IGF1R induced cancer cell death. Previous reports suggest that the stimulation of IGF1R can lead to the activation of at least two signaling pathways involving mitogen-activated protein kinase and AKT under conditions that often require the removal or reduction of other growth factors (Kooijman, 2006; Kurmasheva and Houghton, 2006). Our data show that AKT signaling is specifically affected by anti-IGF1R and a constitutively active *AKT* (myr-*AKT1*) can significantly inhibit h7C10-mediated AKT inhibition and RMS cell death. The results suggest that the AKT pathway is the primary signaling cascade inhibited by anti-IGF1R, which is important for cell survival in the sensitive RMS cells, without any evidence of mitogen-activated protein kinase involvement.

AKT has been implicated in cell survival via multiple pathways (Manning and Cantley, 2007) including: (1) phosphorylation and subsequent inhibition of BAD; (2) blocking FOXO-mediated activation of target genes that promote apoptosis; (3) inhibiting MDM2 that triggers the degradation of p53; and (4) activating NFκB survival signal. Of the targets regulated by AKT, BAD is particularly relevant to IGF1R-mediated survival signaling in protecting IL-3-dependent hemopoietic cells from IL-3 withdrawal (Peruzzi *et al.*, 1999). Moreover, BAD was shown to specifically interact with and counter the death inhibition mediated by Bcl-x_L, but not Bcl-2, via releasing free BAX (Yang *et al.*, 1995). Our results show that the sensitive cells with elevated IGF1R are negative for Bcl-2 and the treatment with h7C10 results in hypophosphorylated BAD and activated BAX. In addition, the ectopic

expression of Bcl-x_L leads to resistance of h7C10-induced apoptosis in Rh41 cells. Further, RNA interference against Bcl-x_L results in sensitizing Bcl-2 negative CTR cells to h7C10-induced apoptosis, with little effect on Bcl-2 positive RD cells. Our results suggest that the ability of anti-IGF1R to induce RMS cell death is in part mediated through Bcl-x_L.

Our data also shows that anti-IGF1R can induce cell death and inhibit cell growth in the same cancer cells. By increasing the level of Bcl-x_L in Rh41 cells via gene transfer, one can effectively prevent anti-IGF1R induced apoptosis. However, the Bcl-x_L overexpressing cells are still very much susceptible to anti-IGF1Rinduced growth arrest. Such dependence on extrinsic signals was previously described in IL-3-dependent lymphocytes where the expression of Bcl-x_L prevented cell death, but not atrophy following IL-3 withdrawal (Rathmell *et al.*, 2000). The results indicate that IGF1R has evolved to be crucial for some RMS by promoting both growth and survival, a single event resulting in a clear advantage for RMS pathogenesis.

As tumor regression is the best clinical end point for early stage studies, it is therefore important to identify rational biomarkers that can be implemented in clinical correlative studies. Our results show an inverse correlation between elevated IGF1R and Bcl-2 overexpression in both RMS cell lines and tumors. More importantly, the most responsive cell lines (Rh41, Rh4 and CTR) are Bcl-2 negative. Based on the absence of Bcl-2 in the h7C10 sensitive cells and roles of AKT and Bcl-x_L in h7C10 induced cell death in the RMS cells, we suggest that the role of elevated IGF1R is to inactivate BAD, and thus allowing Bcl-x_L to suppress cell death, thereby circumventing the need to overexpress Bcl-2. It will be particularly interesting to follow-up with clinical correlative studies on the expression of Bcl-2 and the response to IGF1R targeted therapies.

In summary, we present here a preclinical model for the evaluation of IGF1R targeted therapies, in which anti-IGF1R induces cell death in the complete culture medium and rapid tumor regression in xenograft mice. The analysis of the mechanism for IGF1R antibody-induced cell death reveals mitochondrial-dependent apoptosis, involving the activation of BAD and BAX. Our data also illustrates an inverse correlation between elevated IGF1R and Bcl-2 expression in RMS, and anti-IGF1R induced cell death is limited to some RMS cells negative for Bcl-2. Further, the transgenic expression of myr-AKT and pro-survival Bcl-x_L inhibit anti-IGF1R-induced apoptosis, whereas the downregulation of Bcl-x_L sensitizes Bcl-2 negative cells to anti-IGF1R. Thus, our results suggest that elevated IGF1R promotes cell survival via a process involving AKT and Bcl-x_L, in some cancer cells negative for Bcl-2. Our investigation outlines a mechanism of action and relevant biomarkers for clinical correlative studies to assess tumor regression in response to anti-IGF1R agents.

Materials and methods

Cell lines and reagents

All human RMS cell lines, RD, Rh1, Rh4, Rh18, Rh28, Rh30, Rh41, Rh36, CTR and RMS13 were maintained in RPMI-1640 with 10% fetal bovine serum and antibiotics. Mock control antibody MOPC 21 was from Sigma (St Louis, MO, USA), and anti-IGF1R antibody h7C10 was kindly provided by Merck. The control and *Bcl-x_L* lentiviruses, pHAGE-CMV-MCS-IZsGreen-W (green fluorescence protein (GFP)-Ctrl) and pIZsGreenW-*Bcl-x_L* (GFP-Bcl-x_L) were provided by Dr Andrius Kazlauskas (Barcia *et al.*, 2007). Rh41 cells were infected with GFP-Ctrl or GFP-*Bcl-x_L* lentiviruses. Approximately 60–100% cells were GFP positive following infection. Post-infection, the cells were FACS sorted for GFP positive cells. Myr-*AKT1* and control adenoviruses were obtained from Vector Biolabs (Philadelphia, PA, USA). Rh41 were infected by the adenoviruses at MOI of 20 for 2 days,

followed by the analysis of intracellular proteins and sensitivity to h7C10. Anonymous human RMS tumors were obtained from patients at US National Cancer Institute.

Cell viability and clonogenic assays

Cell proliferation assays were performed with ATPLite reagent (PerkinElmer, Waltham, MA, USA) as previously described (Cao *et al.*, 2008). All experiments were performed in triplicate and at least three repetitive experiments were performed for each result. Live cell counting was performed in triplicate using NucleoCounter (New Brunswick Scientific, Edison, NJ, USA) or Cellometer (Nexcelom Biosciences, Lawrence, MA, USA) per the manufacturer's protocol to determine the percentage of live cells. For cell proliferation assays performed with crystal violet, cells were fixed with 4% glutaraldehyde, stained with 0.1% crystal violet in 1% EtOH, washed and dried. The dye was extractioned using 10% acetic acid and measured using a Victor plate reader (PerkinElmer) at 560 nm. Clonogenic assays were performed with 0.5% crystal violet (Franken *et al.*, 2006). All clonogenic experiments were reproduced.

Human tissues and animal studies

Anonymous human RMS tumor and control skeletal muscle tissues were obtained from patients at the US National Cancer Institute. Animal protocol was approved by NCI Animal Care and Use Committee. Female 4–6-week-old severe combined immunodeficiency (SCID) mice were purchased from Charles River Laboratories (Wilmington, MA, USA). The animal study was done as previously described (Cao *et al.*, 2008) except that h7C10 treatment was initiated once tumors reached about 5mm in maximal length (subtracted that of the un-inoculated leg) to determine its ability to induce tumor regression. The drug was give at 10 mg/kg i.p. twice weekly for a total of 3 weeks. Tumors were measure by caliper twice weekly.

Mitochondrial depolarization assay

Rh41 cells (40 000 cells/well) were plated in 4-well chamber slides (LabTek, Nalge Nunc International, Rochester, NY, USA) and treated with h7C10. JC-1 dye was prepared as per the manufacturer's instructions (Invitrogen, Carlsbad, CA, USA; Troiano *et al.*, 2007). Cells were stained with 2.5 μg/ml JC-1 for 30 min at 37 °C. The dye was washed off with PBS and the cells were imaged on a Zeiss 510 NLO confocal microscope. For FACS analysis, Rh41 cells were stained with warm media containing 2.5 μg/ml JC-1 at 37 °C for 15–30 min. After removal JC-1 dye, the cells were resuspended in PBS before processing on BD FACS Calibur (BD Biosciences, San Jose, CA, USA).

Cytochrome C release

Rh41 cells were plated at a density of either 2.5×10^6 cells per 10 cm dish or 5.0×10^6 cells per 15 cm dish. One day after plating, the cells were treated with 10 μg/ml h7C10 for the time periods noted in the figure legends. Post-treatment, cells were harvested and processed for mitochondrial and cytosolic fractionation as described (Phillips *et al.*, 2007). Cytosolic and mitochondrial fractions were analyzed by immunoblots.

Activated Bax immunoprecipitation

Rh41 cells were plated at 2.5×10^6 cells per 10 cm dish. They were treated with 10 μg/ml h7C10 antibody for 24 h, or 1 μM staurosporine for 4 h. The cells were permeabilized with 100 μg/ml digitonin and the supernatant containing the cytosolic proteins was removed and the remaining cell pellet containing mitochondrial proteins was solubilized with CHAPS buffer, precleared and immunoprecipitated with a monoclonal BAX antibody that recognize

oligomerized BAX (BD Biosciences) as described (Phillips *et al.*, 2007). The precipitated proteins were resuspended in 100 μl of 1× sample buffer and analyzed by immunoblots.

Immunoblots and electrochemiluminescence assays

Cell and tissue lysates were prepared as previously described (Cao *et al.*, 2008). The antibodies against ERK, p-ERK (Thr202/Tyr204), AKT and p-AKT (Ser473; Thr308), p-4EBP1 (Thr37/46), p-mTOR (Ser2481), p-GSK-3β (Ser21/9), p-S6RP (Ser240/244), BAD, p-BAD (Ser112), Bcl-2, Bcl-x_L, BAK, voltage-dependent anion channel, Casp-3, Casp-9, GAPDH and actin were obtained from Cell Signaling Technology (Danvers, MA, USA). The cytochrome C and Bax monoclonal antibodies were from BD Pharmingen. IGF1R immunoassay was performed as previously described (Cao *et al.*, 2008).

FACS analysis of apoptotic cells with Apo-5-bromo-2-deoxyuridine staining

One day after plating (1×10^6 cells per 10 cm dish), cells were treated with 10 μg/ml h7C10 for the time periods indicated in the figure legends. After treatment, cells were harvested and processed using the Apo-BrdU Flow Cytometry kit (BD Biosciences) according to the manufacturer's protocols.

RNA interference experiments for Bcl-x_L

Cells were transfected in 6-well plates with 80 pmol small interfering RNA and 4 μl oligofectamine for Bcl-x_L (5′-GAUACAGCUGGAGUCAGUUUAGUGA-3′, Invitrogen) or control for two days. The cell lysates were analyzed for the expression of Bcl-x_L via immunoblots. The transfected cells were then plated and treated with h7C10 for 2 days and the fraction of dead cells was determined with trypan blue staining via Cellometer (Nexcelom Biosciences).

Statistical analysis

Statistical analyses were performed with Prism (GraphPad). All cell-based studies were done in triplicate. Data were presented as mean ± s.e.m. Statistical comparisons were determined with Student's *t*-test, Fisher's exact test or two-way ANOVA test using Prism. Statistical significance was defined as $P < 0.05$.

Acknowledgments

We thank Dr Andrius Kazlauskas for providing the lentivirus expressing Bcl-x_L, and Arnulfo Mendoza, Vanessa Moore, Susan Garfield and Barbara Taylor for excellent technical assistance. This research was supported by the Intramural Research Program of the US National Cancer Institute (NCI). This project was also funded in part with federal funds from the NCI, NIH, under contract N01-CO-12400.

References

Adams JM, Cory S. The Bcl-2 apoptotic switch in cancer development and therapy. Oncogene. 2007; 26:1324–1337. [PubMed: 17322918]

Barcia RN, Dana MR, Kazlauskas A. Corneal graft rejection is accompanied by apoptosis of the endothelium and is prevented by gene therapy with bcl-xL. Am J Transplant. 2007; 7:2082–2089. [PubMed: 17614980]

Burtrum D, Zhu Z, Lu D, Anderson DM, Prewett M, Pereira DS, et al. A fully human monoclonal antibody to the insulin-like growth factor I receptor blocks ligand-dependent signaling and inhibits human tumor growth *in vivo*. Cancer Res. 2003; 63:8912–8921. [PubMed: 14695208]

Cao L, Yu Y, Darko I, Currier D, Mayeenuddin LH, Wan X, et al. Addiction to elevated insulin-like growth factor I receptor and initial modulation of the AKT pathway define the responsiveness of rhabdomyosarcoma to the targeting antibody. Cancer Res. 2008; 68:8039–8048. [PubMed: 18829562]

Clemmons DR. Modifying IGF1 activity: an approach to treat endocrine disorders, atherosclerosis and cancer. Nat Rev Drug Discov. 2007; 6:821–833. [PubMed: 17906644]

Cohen BD, Baker DA, Soderstrom C, Tkalcevic G, Rossi AM, Miller PE, et al. Combination therapy enhances the inhibition of tumor growth with the fully human anti-type 1 insulin-like growth factor receptor monoclonal antibody CP-751,871. Clin Cancer Res. 2005; 11:2063–2073. [PubMed: 15756033]

Datta SR, Ranger AM, Lin MZ, Sturgill JF, Ma YC, Cowan CW, et al. Survival factor-mediated BAD phosphorylation raises the mitochondrial threshold for apoptosis. Dev Cell. 2002; 3:631–643. [PubMed: 12431371]

Franken NA, Rodermond HM, Stap J, Haveman J, van Bree C. Clonogenic assay of cells in vitro. Nat Protoc. 2006; 1:2315–2319. [PubMed: 17406473]

Goetsch L, Gonzalez A, Leger O, Beck A, Pauwels PJ, Haeuw JF, et al. A recombinant humanized anti-insulin-like growth factor receptor type I antibody (h7C10) enhances the antitumor activity of vinorelbine and anti-epidermal growth factor receptor therapy against human cancer xenografts. Int J Cancer. 2005; 113:316–328. [PubMed: 15386423]

Gualberto A, Pollak M. Emerging role of insulin-like growth factor receptor inhibitors in oncology: early clinical trial results and future directions. Oncogene. 2009; 28:3009–3021. [PubMed: 19581933]

Haluska P, Shaw HM, Batzel GN, Yin D, Molina JR, Molife LR, et al. Phase I dose escalation study of the anti insulin-like growth factor-I receptor monoclonal antibody CP-751,871 in patients with refractory solid tumors. Clin Cancer Res. 2007; 13:5834–5840. [PubMed: 17908976]

Hennessy BT, Smith DL, Ram PT, Lu Y, Mills GB. Exploiting the PI3K/AKT pathway for cancer drug discovery. Nat Rev Drug Discov. 2005; 4:988–1004. [PubMed: 16341064]

Jiang X, Wang X. Cytochrome C-mediated apoptosis. Annu Rev Biochem. 2004; 73:87–106. [PubMed: 15189137]

Kooijman R. Regulation of apoptosis by insulin-like growth factor (IGF)-I. Cytokine Growth Factor Rev. 2006; 17:305–323. [PubMed: 16621671]

Kurmasheva RT, Houghton GB. IGF-I mediated survival pathways in normal and malignant cells. Biochim Biophys Acta. 2006; 1766:1–22. [PubMed: 16844299]

Manning BD, Cantley LC. AKT/PKB signaling: navigating downstream. Cell. 2007; 129:1261–1274. [PubMed: 17604717]

Minshall C, Arkins S, Straza J, Conners J, Dantzer R, Freund GG, et al. IL-4 and insulin-like growth factor-I inhibit the decline in Bcl-2 and promote the survival of IL-3-deprived myeloid progenitors. J Immunol. 1997; 159:1225–1232. [PubMed: 9233617]

Muslin AJ, Tanner JW, Allen PM, Shaw AS. Interaction of 14-3-3 with signaling proteins is mediated by the recognition of phosphoserine. Cell. 1996; 84:889–897. [PubMed: 8601312]

Parrizas M, LeRoith D. Insulin-like growth factor-1 inhibition of apoptosis is associated with increased expression of the bcl-xL gene product. Endocrinology. 1997; 138:1355–1358. [PubMed: 9048647]

Peruzzi F, Prisco M, Dews M, Salomoni P, Grassilli E, Romano G, et al. Multiple signaling pathways of the insulin-like growth factor 1 receptor in protection from apoptosis. Mol Cell Biol. 1999; 19:7203–7215. [PubMed: 10490655]

Phillips DC, Martin S, Doyle BT, Houghton JA. Sphingosine-induced apoptosis in rhabdomyosarcoma cell lines is dependent on pre-mitochondrial Bax activation and post-mitochondrial caspases. Cancer Res. 2007; 67:756–764. [PubMed: 17234787]

Rathmell JC, Vander Heiden MG, Harris MH, Frauwirth KA, Thompson CB. In the absence of extrinsic signals, nutrient utilization by lymphocytes is insufficient to maintain either cell size or viability. Mol Cell. 2000; 6:683–692. [PubMed: 11030347]

Rodriguez-Tarduchy G, Collins MK, Garcia I, Lopez-Rivas A. Insulin-like growth factor-I inhibits apoptosis in IL-3-dependent hemopoietic cells. J Immunol. 1992; 149:535–540. [PubMed: 1624800]

Sachdev D, Li SL, Hartell JS, Fujita-Yamaguchi Y, Miller JS, Yee D. A chimeric humanized single-chain antibody against the type I insulin-like growth factor (IGF) receptor renders breast cancer cells refractory to the mitogenic effects of IGF-I. Cancer Res. 2003; 63:627–635. [PubMed: 12566306]

Shimizu S, Narita M, Tsujimoto Y. Bcl-2 family proteins regulate the release of apoptogenic cytochrome c by the mitochondrial channel VDAC. Nature. 1999; 399:483–487. [PubMed: 10365962]

Tolcher AW, Sarantopoulos J, Patnaik A, Papadopoulos K, Lin CC, Rodon J, et al. Phase I, pharmacokinetic, and pharmacodynamic study of AMG 479, a fully human monoclonal antibody to insulin-like growth factor receptor 1. J Clin Oncol. 2009; 27:5800–5807. [PubMed: 19786654]

Troiano L, Ferraresi R, Lugli E, Nemes E, Roat E, Nasi M, et al. Multiparametric analysis of cells with different mitochondrial membrane potential during apoptosis by polychromatic flow cytometry. Nat Protoc. 2007; 2:2719–2727. [PubMed: 18007607]

Wang Y, Hailey J, Williams D, Wang Y, Lipari P, Malkowski M, et al. Inhibition of insulin-like growth factor-I receptor (IGF1R) signaling and tumor cell growth by a fully human neutralizing anti-IGF1R antibody. Mol Cancer Ther. 2005; 4:1214–1221. [PubMed: 16093437]

Wu JD, Odman A, Higgins LM, Haugk K, Vessella R, Ludwig DL, et al. *In vivo* effects of the human type I insulin-like growth factor receptor antibody A12 on androgen-dependent and androgen-independent xenograft human prostate tumors. Clin Cancer Res. 2005; 11:3065–3074. [PubMed: 15837762]

Yaffe MB, Rittinger K, Volinia S, Caron PR, Aitken A, Leffers H, et al. The structural basis for 14-3-3:phosphopeptide binding specificity. Cell. 1997; 91:961–971. [PubMed: 9428519]

Yang E, Zha J, Jockel J, Boise LH, Thompson CB, Korsmeyer SJ. Bad, a heterodimeric partner for Bcl-XL and Bcl-2, displaces Bax and promotes cell death. Cell. 1995; 80:285–291. [PubMed: 7834748]

Zha J, Harada H, Yang E, Jockel J, Korsmeyer SJ. Serine phosphorylation of death agonist BAD in response to survival factor results in binding to 14-3-3 not BCL-X(L). Cell. 1996; 87:619–628. [PubMed: 8929531]

Zhang J, D'Ercole AJ. Expression of Mcl-1 in cerebellar granule neurons is regulated by IGF-I in a developmentally specific fashion. Brain Res Dev Brain Res. 2004; 152:255–263.

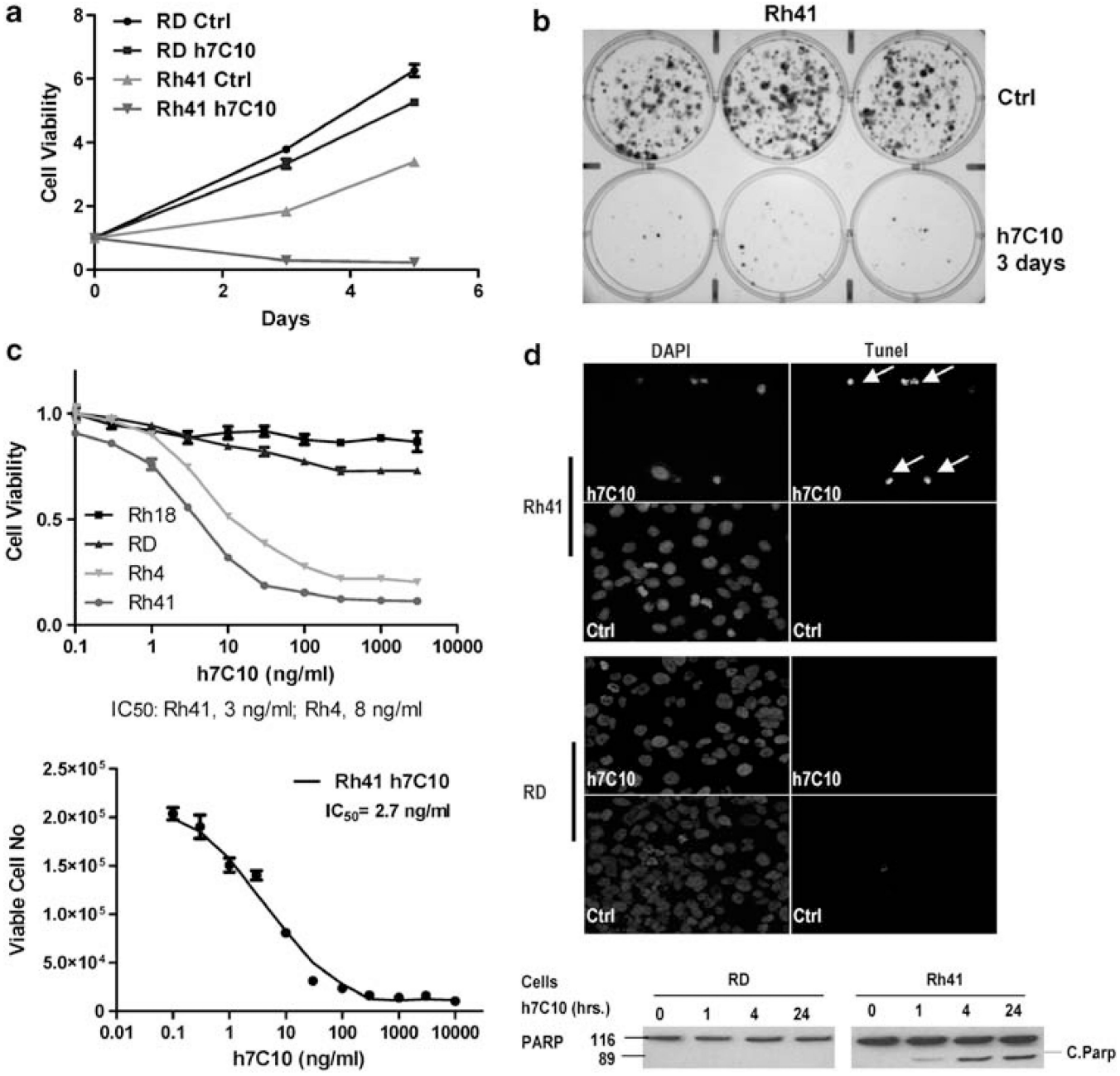

Figure 1.

Anti-IGF1R antibody h7C10 induces RMS cell death. (**a**) Growth analysis of RMS cell lines treated with h7C10 or mock antibody, followed by ATPLite assay. (**b**) Sensitive Rh41 cells were treated with h7C10 for 3 days. The antibody was replaced with fresh medium for 2 weeks for clonogenic assay. (**c**) Dose effects of h7C10 on selected RMS cells. Cells were treated with indicated concentrations of h7C10 for 3 days, followed by ATPLite assay, or by direct counting for viable cells (bottom). Data are shown as mean ± s.e.m. ($n = 3$). (**d**) RMS cells were treated with h7C10 for two days or indicated time, and analyzed with Tunel assay or immunoblot for PARP. All h7C10 treatment was done at 10 μg/ml unless otherwise indicated. The arrows are indicative of Tunel positive apoptotic cells. DAPI, 4′-6-diamidino-2-phenylindole.

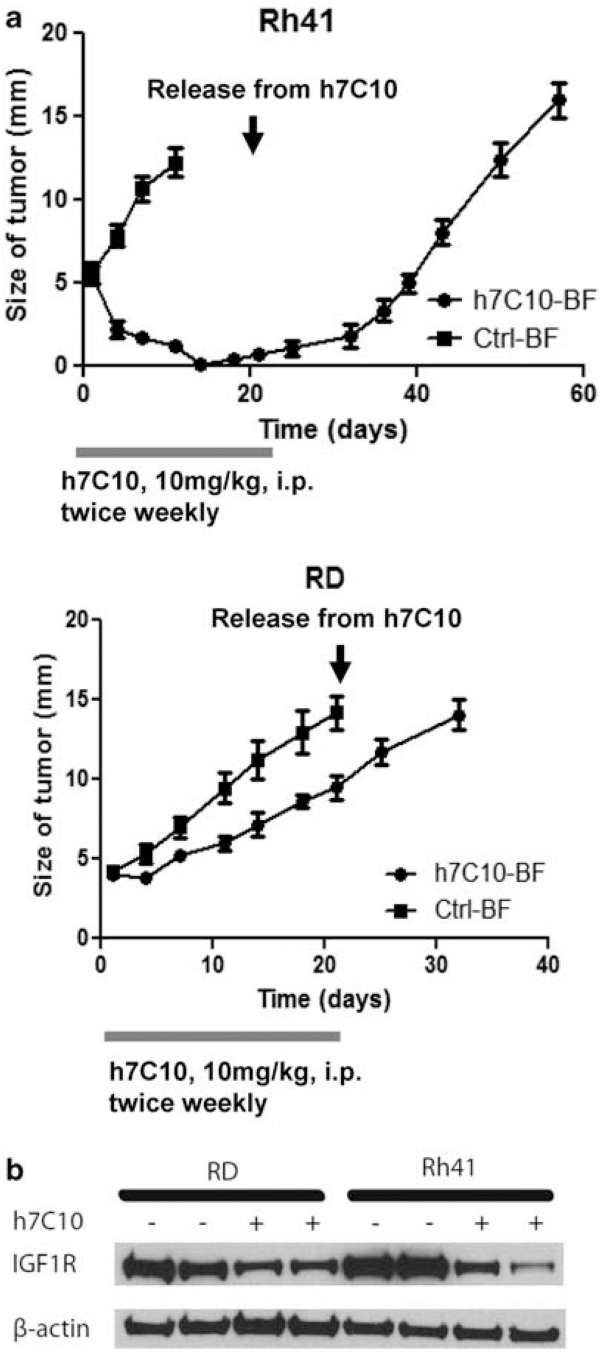

Figure 2.

h7C10 leads to selective regression of Rh41 tumors. (**a**) Rh41 and RD cells were inoculated intramuscularly into the leg of SCID mice ($n = 10$). When the tumors reached 5mm in size with back-to-front (BF) measurement (subtracted that of the un-inoculated leg), h7C10 was injected i.p. at 10 mg/kg twice weekly for a total of 3 weeks as indicated. The sizes of the tumors were measured with caliper twice weekly. (**b**) After 4 days of h7C10 treatment, tumors were obtained and their lysates were used for immunoblot to verify IGF1R downregulation.

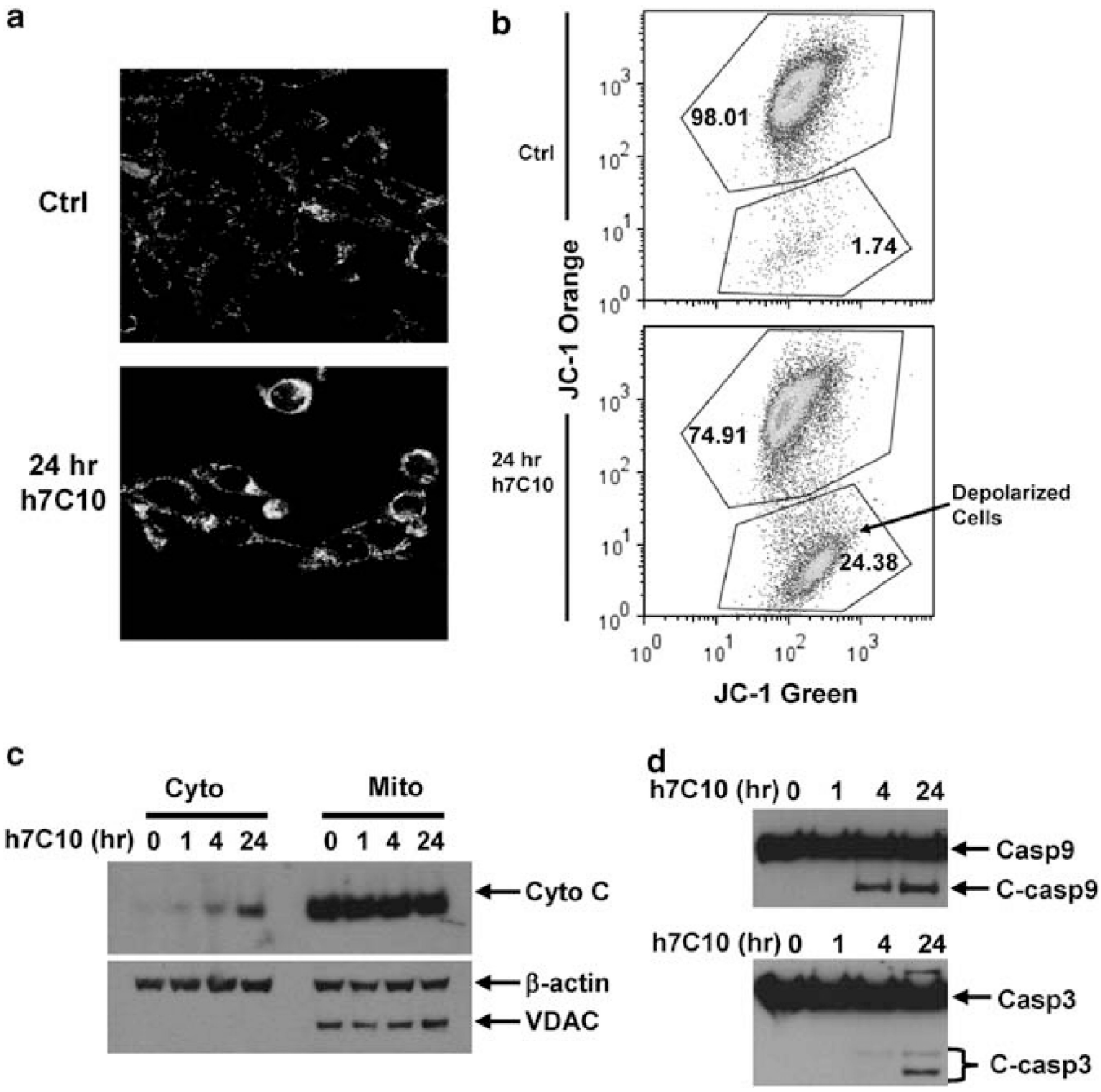

Figure 3.

The h7C10-induced apoptosis is mediated through mitochondrial depolarization. (**a**) Rh41 cells were treated with h7C10 for 24 h. The cells were stained with mitochondrial membrane potential dye JC-1 and analyzed by confocal microscopy. (**b**) Rh41 cells were treated with h7C10 for 24 h, stained with JC-1 and analyzed with FACS for depolarized population. (**c**) Both cytosolic (cyto) and mitochondrial (mito) fractions were prepared from h7C10 treated Rh41. Immunoblots were carried out to detect the release of cytochrome C into the cytosolic fraction. Voltage-dependent anion channel, a mitochondrial specific ion channel protein, was used as a marker to validate sample fractionation. (**d**) Total cell lysates were prepared

following h7C10 treatment of Rh41, and analyzed for full-length and cleaved caspase 9 and caspase 3.

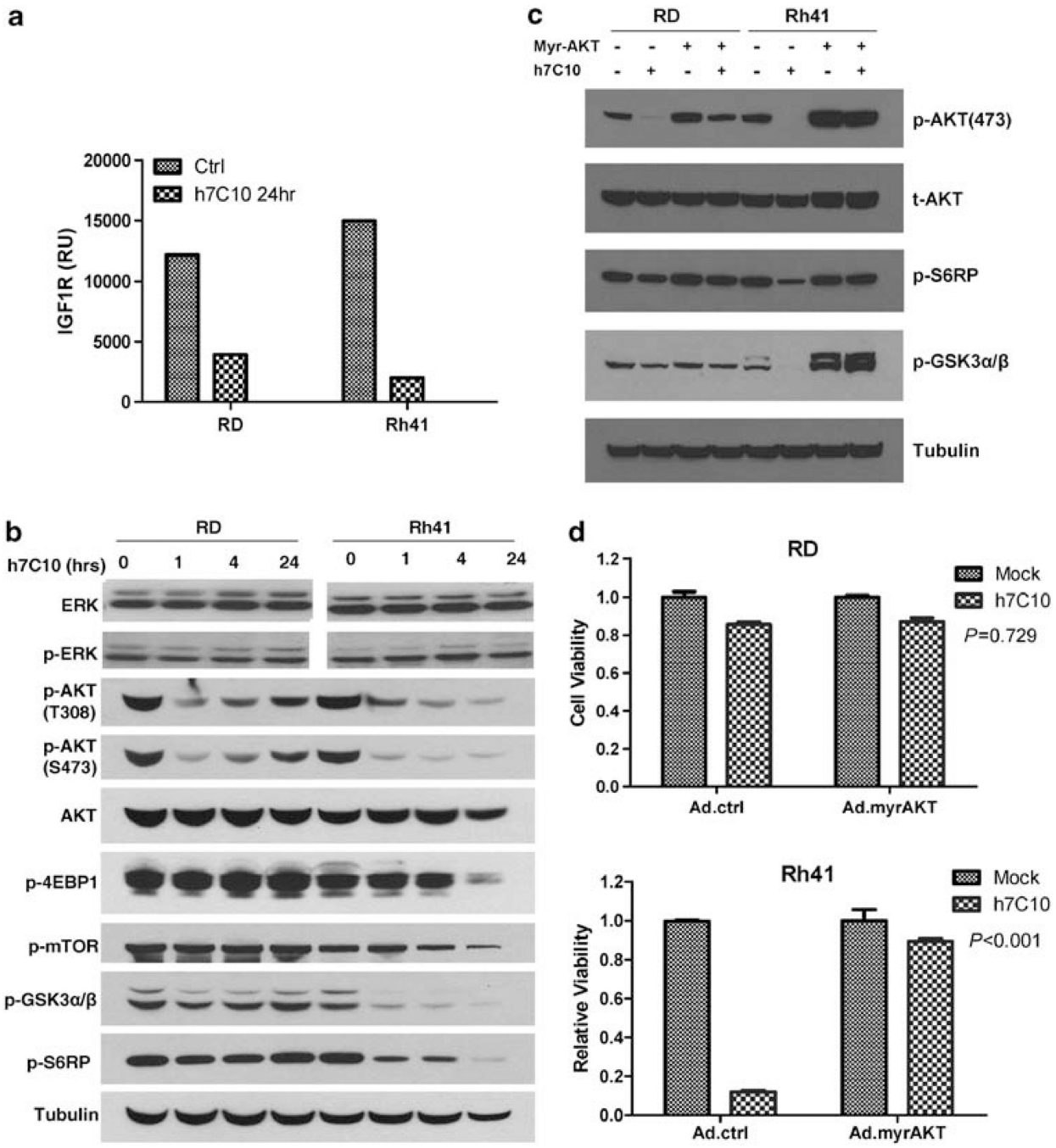

Figure 4.

h7C10 activity involves AKT signaling. (**a**) RMS cells were treated with h7C10 for 24 h. The cell lysates were analyzed with an IGF1R sandwich immunoassay. (**b**) Immunoblots against t/p-ERK, t/p-AKT and AKT downstream targets with cells treated with h7C10 at the indicated time points. (**c**) Cells were infected with myr-*AKT* or control adenovirus for 2 days, followed by h7C10 treatment for 4 h. Immunoblots revealed the restoration of AKT signaling with myr-AKT. (**d**) myr-*AKT* adenovirus infected cells were treated with h7C10 for 2 days and analyzed for viable cells. Statistic interaction *P*-values between h7C10 and myr-*AKT* were determined using two-way ANOVA.

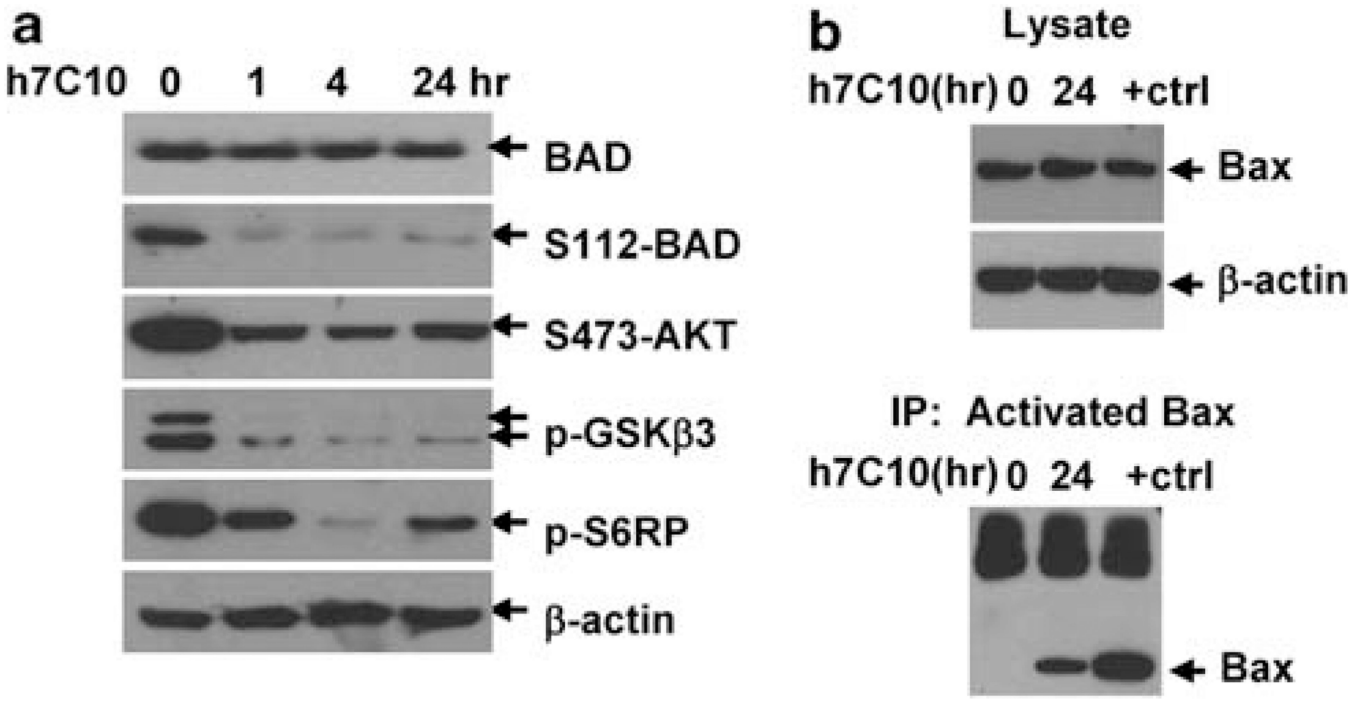

Figure 5.

h7C10 treatment results in the activation of BAD and BAX. (**a**) Rh41 was treated with h7C10 for the indicated time and analyzed with immunoblots against t/p-BAD, as well as other phospho-proteins downstream of AKT signaling. (**b**) Rh41 was treated with h7C10 for 24 h and 1 μM staurosporine (+ctrl) for 4 h. Lysates were made and immunoprecipitated with an antibody against oligomerized BAX (active). Immunoblots were performed with a BAX antibody.

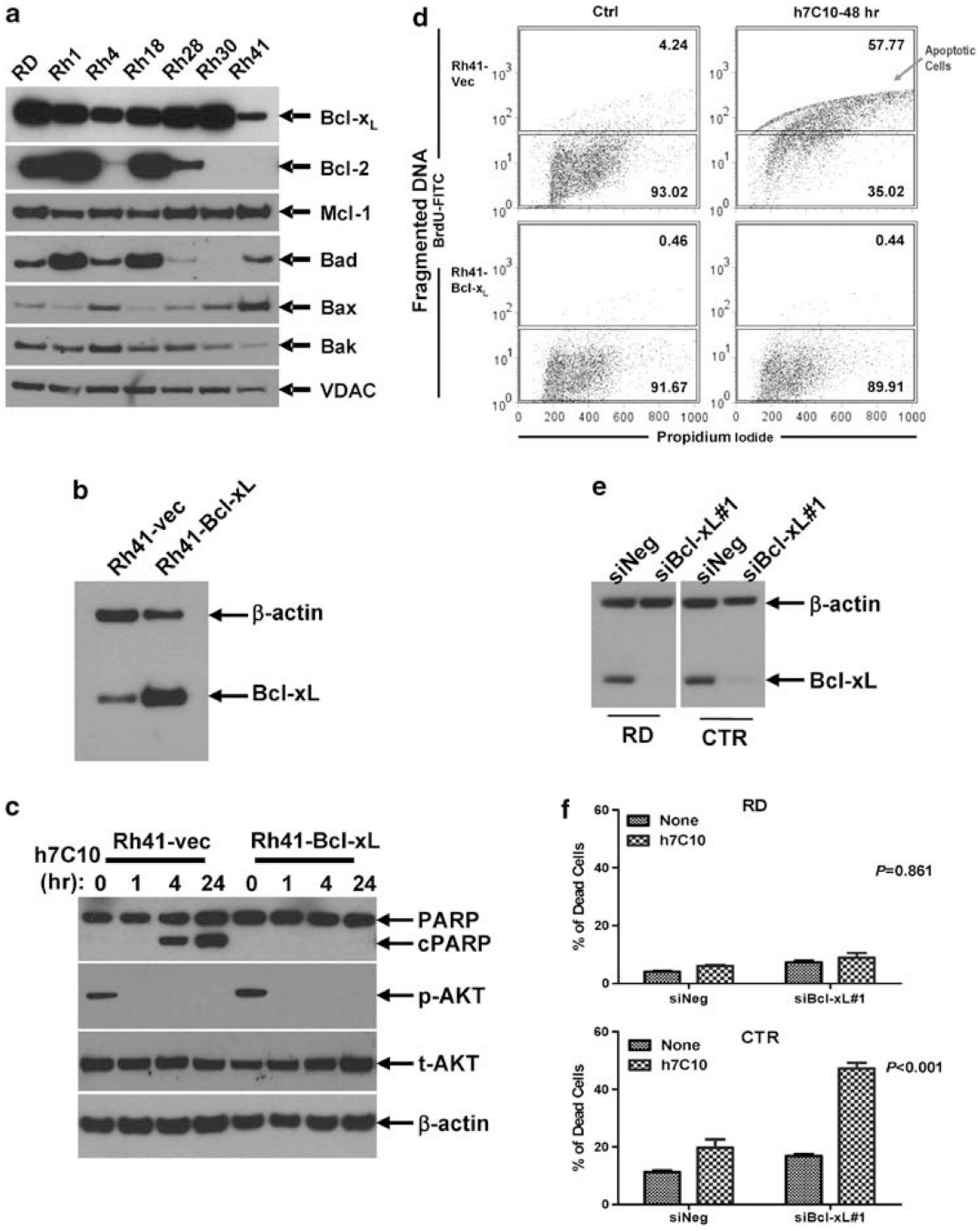

Figure 6.

Involvement of Bcl-x_L in h7C10-induced cell death. (**a**) Analysis of the expression of pro-survival and pro-apoptotic proteins in RMS cell lines. (**b**) Generation of *Bcl-x_L* lentivirus-infected Rh41 cells. Rh41 cells were infected with control and *Bcl-x_L* lentiviruses and sorted with coexpressing GFP via FACS. The expression of Bcl-x_L was verified by immunoblot. (**c**) Rh41-*Bcl-x_L* and vector infected cells were treated with h7C10, lysates were used for the detection of p-AKT and cleaved PARP. (**d**) Rh41-vec and Rh41-*Bcl-x_L* cells were treated with h7C10 for 2 days. The apoptotic cells were labeled with 5-bromo-2-deoxyuridine (BrdU) and analyzed with FACS. Apoptotic cells have increased DNA fragmentation, and

thus elevated BrdU-FITC signal. (**e**) RMS cells were transfected with siBcl-x_L and the lysates were analyzed via immunoblot. (**f**) RMS cells transfected with siBcl-x_L were further treated with h7C10. The percentage of dead cells was determined with cellometer. Statistic interaction *P*-values between h7C10 and siBcl-x_L were determined using two-way ANOVA.

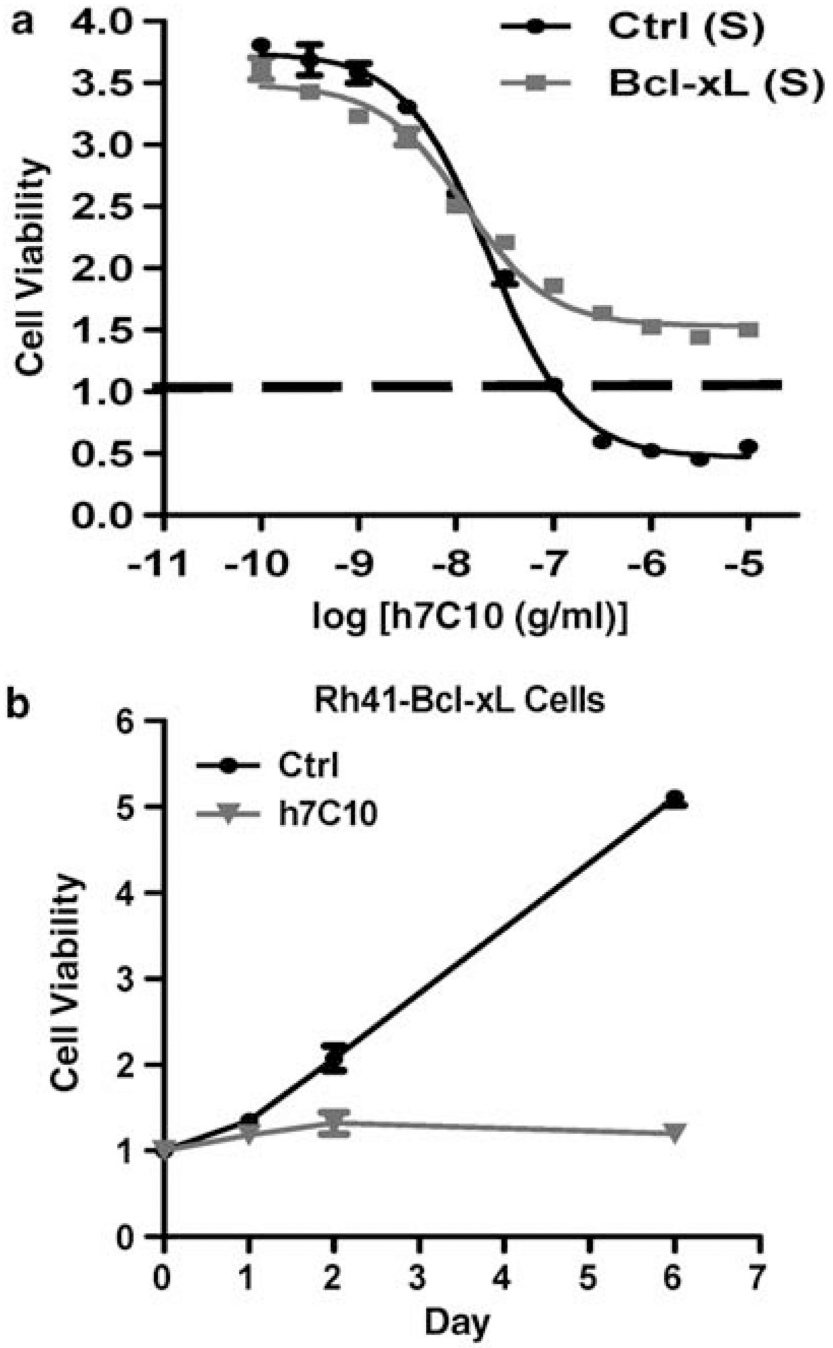

Figure 7.

Overexpression of Bcl-x_L prevents h7C10-induced cell death, but not growth arrest. (a) Both *Bcl-x_L* and vector lentiviruses infected Rh41 cells were treated with h7C10 for 3 days and analyzed for viable cells. Baseline was defined as the readings at the time of h7C10 addition. A number below 1 indicates reduced cells viability. (**b**) Rh41-Bcl-x_L cells were plated in 12-well plates and treated with h7C10 at day 0. Cell proliferation assay was performed with crystal violet staining followed by extraction and quantification at the indicated time points.

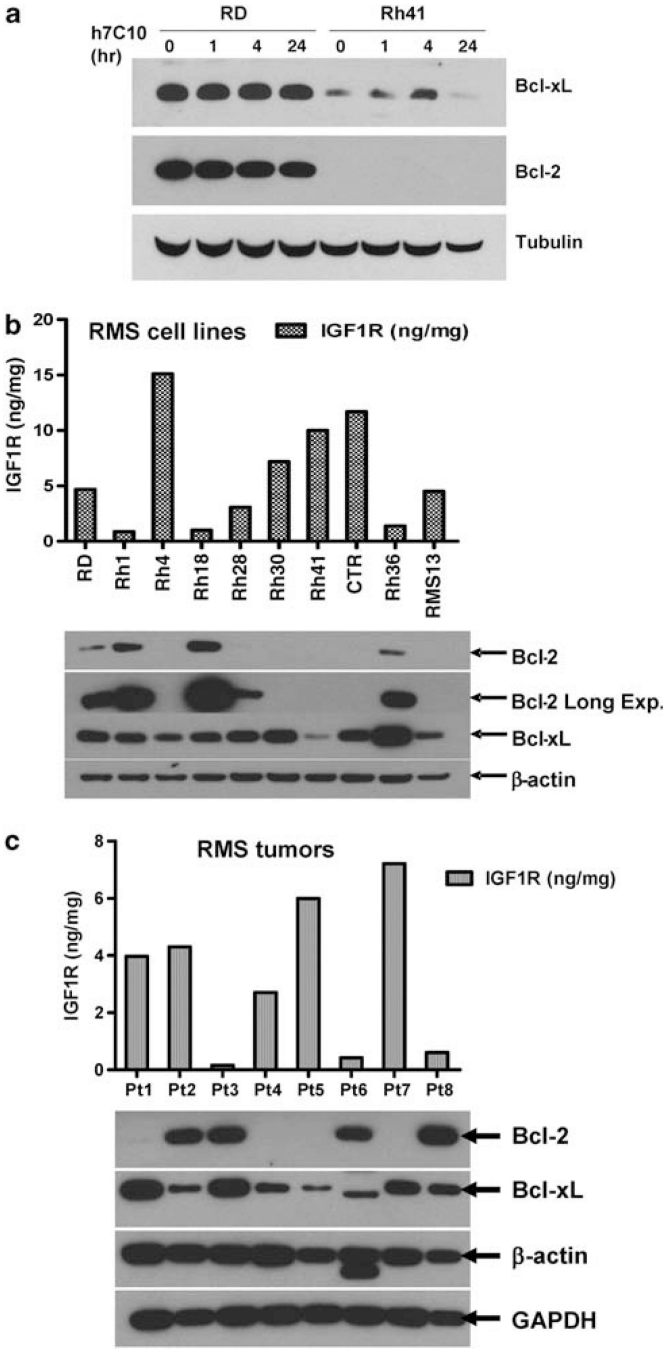

Figure 8.

Correlation between Bcl-2 and IGF1R in RMS cell lines and tumors. (**a**) Effects of anti-IGF1R on Bcl-2 and Bcl-x_L in resistant RD and sensitive Rh41 cells. (**b**) Determination of IGF1R levels with ECL immunoassay and Bcl-2 and Bcl-x_L with immunoblots in RMS cell lines. (**c**) Determination of IGF1R levels with ECL immunoassay and Bcl proteins with immunoblots in RMS tumors.